

## **General Disclaimer**

### **One or more of the Following Statements may affect this Document**

- This document has been reproduced from the best copy furnished by the organizational source. It is being released in the interest of making available as much information as possible.
- This document may contain data, which exceeds the sheet parameters. It was furnished in this condition by the organizational source and is the best copy available.
- This document may contain tone-on-tone or color graphs, charts and/or pictures, which have been reproduced in black and white.
- This document is paginated as submitted by the original source.
- Portions of this document are not fully legible due to the historical nature of some of the material. However, it is the best reproduction available from the original submission.

X-616-69-124

NASA TM X-7 63508

# THE MAGNETIC FIELD OF THE MAGNETOSPHERE AND TAIL

D. H. FAIRFIELD

N 69-22157

FACILITY FORM 602

(ACCESSION NUMBER)

47

(PAGES)

TMX 63508

(NASA CR OR TMX OR AD NUMBER)

(THRU)

(CODE)

29

(CATEGORY)

APRIL 1969

**GSFC**

**GODDARD SPACE FLIGHT CENTER**  
**GREENBELT, MARYLAND**

X-616-69-124

THE MAGNETIC FIELD OF THE MAGNETOSPHERE AND TAIL

D. H. Fairfield  
Laboratory for Space Sciences  
NASA-Goddard Space Flight Center  
Greenbelt, Maryland USA

April 1969

Extraterrestrial Physics Branch Preprint Series

---

Review paper presented at the NATO Advanced Study Institute on  
Production and Maintenance of the Polar Ionosphere in Tretten,  
Norway. Proceedings to be published by Gordon and Breach.

## Abstract

Earth orbiting spacecraft have made extensive measurements of the solar wind-compressed magnetic field in the sunward magnetosphere and the extended magnetic field of the geomagnetic tail. Analysis of the measurements indicate that in an average magnetosphere, field lines crossing the earth above  $78^{\circ} \pm 3^{\circ}$  and  $69^{\circ} \pm 2^{\circ}$  geomagnetic latitude in the noon and midnight meridians respectively are extended into the geomagnetic tail. Field lines in the northern and southern hemispheres of the tail are generally oriented parallel or anti-parallel to the earth sun line with the two regions being separated by a neutral sheet or current sheet less than  $1 R_E$  thick. The average field magnitude is  $16\gamma$  at  $20 R_E$  and  $7\gamma$  at  $80 R_E$  except in a region within about  $6 R_E$  of the neutral sheet where the field is depressed by a factor of 2. The observation of tail-like fields almost  $1000 R_E$  behind the earth by the Pioneer 7 spacecraft sets a lower limit on the radial extent of tail associated effects. Departures from the average magnetosphere field configuration occur at the times of magnetic storms and bay events. Storms are associated with higher tail fields and the extension of additional field lines to the tail. Magnetospheric substorms are associated with a relaxation toward a more dipole like configuration. The appearance of electrons near the plasma sheet after bays and the increase in the trapping boundary indicate that field lines may be closed up as high as  $75^{\circ}$  latitude near midnight for brief intervals after substorms.

## I. Introduction

Low-latitude and mid-latitude geomagnetic lines of force are confined by the solar wind to a region within about  $15 R_E$  (earth radii) of the earth known as the magnetosphere. High latitude lines of force are swept downstream from the earth by the solar wind to form the geomagnetic tail which extends some 100's of earth radii in the anti-solar direction. Numerous spacecraft have made measurements in the magnetosphere and tail and the historical development of the subject has been adequately reviewed (see for example, Ness, 1969).

This paper attempts to consolidate current knowledge of the configuration of the magnetic fields of the magnetosphere and tail. Emphasis is placed on the question "what are the paths traced out by magnetic lines of force from different latitudes and longitudes?" Section II reviews work which has integrated large quantities of data and produced an average picture of the magnetosphere and tail. Section III surveys developments which show that variations from the average configuration are quite large and significant. Section IV reviews the high energy particle measurements which yield information about the paths followed by high latitude lines of force. Section V summarizes the findings and Section VI outlines outstanding problems.

## II. Average Magnetic Field Configuration

### 1. The Inner Magnetosphere

Simple theoretical models which include the compressional effects of the solar wind have had considerable success in predicting the configuration of the magnetosphere in the sunward hemisphere. (e.g., Mead, 1964). General hydromagnetic theory has provided some insight into the formation of the geomagnetic tail (see review by Dungey, 1968) but the specific processes taking place at the magnetopause are not sufficiently well understood to input into theoretical model calculations. Simple quantitative model calculations have not had success in predicting the geomagnetic tail. These inadequacies of the theory mean that experimental measurements must take the lead in determining the configuration of the magnetosphere and tail. For this reason the present paper restricts attention to experimental results on the configuration of the magnetosphere and tail. It should be pointed out, however, that quantitative field models have been devised to approximate the experimental results (Williams and Mead, 1965; Taylor and Hones, 1965). Such models are valuable for studies of trapped particles and related effects observed on the ground.

The geomagnetic field inside of 5 earth radii is not greatly distorted by current sources outside the earth's surface except during magnetic storms. Cahill's results (Cahill, 1966) indicate that departures from the dipole field are of the order of 20% at

5  $R_E$  on quiet days. The results of Cummings, et al. (1968) at 6.6  $R_E$  on quiet days show a  $25\gamma \pm 10\gamma$  compression of the field in the sunward hemisphere and a  $5\gamma \pm 10\gamma$  weakening in the night hemisphere relative to an ideal dipole.

With this minimal distortion of the inner magnetosphere in mind, Fairfield (1968a) used the IMP 1, 2 and 3 data taken between 5 and 18  $R_E$  to obtain an experimental determination of the outer magnetosphere. Much of this data from the southern hemisphere is shown projected in the geomagnetic equatorial plane in Figure 1. This figure illustrates the manner in which the magnetic field is swept back toward the tail by the solar wind. The vectors in any one region agree among themselves quite well considering that (1) the data were taken by three spacecraft over a three and one-half year period; (2) data from disturbed intervals were not removed; (3) the measurements were made over a range of latitudes of about  $\pm 70^\circ$ . Since lines of force from the same longitude but different latitudes appeared to be distorted in the same manner it was possible to draw the heavy lines in Figure 1 tangent to the vectors and assume that flux passing through the earth at longitudes between a pair of lines also crossed the equatorial plane between the lines. After constructing experimental contours of constant field strength in the equatorial plane, it was possible to equate dipole flux at the earth's surface to the experimentally determined flux through the equatorial plane. Assuming a dipole

line of force crossing the earth's surface at  $63^{\circ}61'$  latitude and intersecting the equatorial plane at  $5 R_E$ , integration northward in latitude at the earth's surface and outward in the equatorial plane yielded the relation between the latitude of a field line and its equatorial crossing point. This procedure was carried out in each of the  $15^{\circ}$  longitude intervals in the dawn hemisphere and the results are shown in Figure 2. In this view of the magnetosphere equatorial plane the solid lines represent the latitude of the origin of the field lines passing through the equatorial plane at that point. The dashed lines are reproduced from Figure 1 and they represent the longitude of the origin of the field line.

The results of Figure 2 can be used to map phenomena along field lines from the high latitude ionosphere to the equatorial plane. Fairfield mapped the auroral oval determined from ground observations by Feldstein (1963), the region of low altitude magnetic fluctuations observed on a low altitude spacecraft by Zmuda, et al (1967) and a greater than 40 keV electron intensity contour of Frank, et al. (1964). These data are shown in Figure 3. It can be seen that the auroral oval maps to the region of the magnetopause in the sunward hemisphere. In the midnight meridian the last field line that closes within  $10 R_E$  runs to approximately  $68^{\circ}$  latitude. This average magnetosphere suggests that aurora often occur on closed field lines.



Views in meridian planes are shown here as Figure 4. These views incorporate all of the available data from the  $15^\circ$  meridian section of Figure 1 which were taken when the sun was below the geomagnetic equatorial plane. Data are shown projected on the curved sections of Figure 1. The heavy lines were drawn with the aid of the vectors and information of Figure 2 and represent distorted lines while the dashed lines represent dipole lines. Considerable compression of the fields is evident at 0800 but by 0500 the field is quite extended in a tail-like configuration.

The comparable view of the noon-midnight meridian plane is shown as Figure 5. The outermost closed field line in the noon meridian is seen to cross the earth at about  $78^\circ$  latitude with higher latitude lines going back into the tail. One hourly average vector near  $X=5$ ,  $Z=8$  illustrates this turning back of the field.

## 2. The Geomagnetic Tail Within $80 R_E$

Early observations of the geomagnetic tail within  $32 R_E$  of the earth with the IMP 1 spacecraft (Ness, 1965) have now been extended beyond the orbit of the moon at  $60 R_E$  (Ness, et al., 1967a; Behannon, 1968; Mihalov, et al., 1968) and even to  $1000 R_E$  (Ness, et al., 1967b; Wolf et al., 1967). Figure 6 reproduces figures of Behannon (1968) showing Explorer 33 hourly average vector measurements in the tail region out to  $80 R_E$ . In the top view vectors are projected in the solar magnetospheric XZ plane

(X axis along the earth-sun line, Z in the plane formed by the X axis and the dipole axis and Y forming a right hand orthogonal system) with the sun at the left and the northern hemisphere at the top of the page. Field lines originating from the south polar cap point away from the earth in the southern hemisphere while field lines connecting to the north polar cap point toward the earth in the northern hemisphere. A neutral sheet or current sheet less than  $1 R_E$  thick (Speiser and Ness, 1967) separates these regions and is located near the solar magnetospheric XY plane. Figure 6 also shows vectors projected into the XY plane when the measurements are made in the northern hemisphere (middle view) and the southern hemisphere (bottom view). The magnetic field of the tail is usually very quiet, especially in regions away from the neutral sheet. The field is invariably oriented near the earth-sun line, but Mihalov, et al. (1968) detect a slight skewing of the field away from this orientation which corresponds to an additional field component in the -Y direction. Behannon (1969) reports an average tail orientation  $3.3^\circ$  from the sun-earth line which could be produced by motion of the earth and collimation of the tail by a 520 km/sec radial solar wind. If flow is actually from east of the sun as is indicated (Brandt, et al., 1969) Behannon's aberration corresponds to a lower and very reasonable solar wind velocity.

Figure 7 (Behannon, 1968) illustrates the radial magnitude gradient of the tail as determined from 256 hours of data from Explorer 33. Data is restricted to quiet periods defined by the

conditions that the geomagnetic activity index  $K_p \leq 2$ . Measurements taken in the weak field region near the neutral sheet were also omitted. The dashed lines in the figure represent the equations  $F \sim (X_{SE})^a$  with  $a = -.5$  for the upper curve at  $X_{SE} = -10$  and  $a = -.1$  for the lower curve. Mihalov, et al. (1968) report results also derived from observations on Explorer 33 which are consistent with Behannon. Mihalov, et al. found no statistically significant radial gradient when using the half of their data sample beyond  $58 R_E$ . The radial gradient can be explained by field lines closing across the neutral sheet or by an expansion in the cross-section of the tail. Behannon (1968) suggests that both effects are important. Mihalov, et al. investigate the field component across the neutral sheet at the time of field reversals and find cases of both northerly and southerly directed fields. The northerly components are more frequent and the southerly components occur almost exclusively beyond  $35 R_E$ .

Figure 8 illustrates recent work by Behannon (1969) demonstrating the existence of a region of depressed field magnitude near the solar magnetospheric equatorial plane. The data consist of 1346 hourly average field magnitudes from Explorers 33 and 35 from 1966-1968 observed at positions  $-70 \leq X_{SM} \leq -20$  at times with  $K_p \leq 2$ . Individual hourly averages were computed by averaging instantaneous measurements of the field magnitude. The average of the hourly values are plotted in the top portion of the figure for each  $2 R_E$  interval of  $Z_{eq}$ . The RMS deviation computed from the hourly average values is shown in the lower portion of the

figure. The fact that the RMS values are not higher in the depressed field region suggests that there exists a broad depressed field region several  $R_E$  thick rather than a thinner low field region which moves throughout the interval of low  $Z_{SM}$ . This broad depressed field region agrees quite well with the expected plasma sheet which has been measured by Vela spacecraft near  $17 R_E$  (Bame, et al., 1967). The existence of a region of depressed field near the equatorial plane and increased field at high latitudes in the midnight sector between 5 and  $11 R_E$  has been emphasized by Heppner, et al. (1967).

Behannon has also obtained the most comprehensive information on the area of the cross-section of the tail in the downstream region (Behannon, 1968, 1969). A figure from his later work is presented as Figure 9. The line segments in this figure represent the trajectory of Explorers 33 and 35 during intervals when they made observations of the tail boundary in the region  $-70 \leq X_{SM} \leq -50 R_E$ . A dashed circle of  $23.5 R_E$  radius has been drawn with its center at  $Y = +3.5$  which corresponds to the line through the center of the tail making an angle of  $3.3^\circ$  with the earth-sun line. The observance of boundary positions  $30 R_E$  south of the solar magnetospheric equatorial plane suggests that the cross-section of the tail is elliptical with the semi-major axis oriented along the solar magnetospheric Z axis. This elongation of the tail is not surprising if one considers the tail as formed by two

approximately circular bundles of flux from the polar caps aligned adjacent to one another.

### 3. The Extended Geomagnetic Tail

Observations of the geomagnetic tail have been obtained by Pioneer 7 passing behind the earth near  $1000 R_E$  (Ness, et al., 1967b; Wolfe, et al., 1967; Fairfield, 1968b) and Pioneer 8 near  $500 R_E$  (Mariani and Ness, 1969). The observations at these distances are similar to one another in that tail-like fields are observed for short intervals of a few minutes to a few hours. Pioneer 7 at  $1000 R_E$  observed the tail approximately 7% of the time during an 11 day interval while Pioneer 8 near  $500 R_E$  observed the tail approximately 25% of the time over a 9 day period. Tail observations at these large distances contrast to the measurements nearer the earth primarily in that (1) the intervals of observation are much shorter in the far downstream region; and (2) the plasma measured in the far downstream tail does not disappear to the extent that it does nearer the earth (Wolfe, et al., 1967).

An example of 2 hours of Pioneer 7 data are illustrated in Figure 9 (Ness, 1969). Two intervals 1633-1656 and 1734-1744 are shown where the field aligned itself with the earth-sun line ( $\phi=180$  or  $360$  and  $\theta=0^\circ$ ). During these two intervals a preliminary comparison with the plasma experiment of the Massachusetts Institute of Technology showed decreased or absent plasma as noted. At 1739 a neutral sheet-like crossing occurred with the field reversing polarity in the manner frequently seen nearer the earth.

The nature of the tail hundreds of  $R_E$  behind the earth is not entirely clear from these measurements of the field at isolated points. Mariani and Ness (1969) interpret the short duration of the tail-like intervals as evidence that the tail is broken up into isolated filaments. Fairfield (1968b) suggests that motion of a well collimated coherent tail in response to the varying direction of the solar wind is an equally good explanation of the observations.

### III. Magnetosphere Time Variations

Although a rather good description exists for an average magnetosphere and tail, it is important to inquire into how often this average configuration corresponds to an actual configuration, and in what respects are the two different. The actual magnetospheric configuration is most apt to correspond to the average experimental configuration during the moderately disturbed periods which occur most frequently and therefore contribute strongly to the average magnetosphere. The greatest deviations from the average condition undoubtedly occur during magnetic storms.

#### 1. Effects of the Main Phase Magnetic Storm

The outstanding characteristic of magnetic storms is the creation of a ring current (Cahill, 1966) which is due to protons (energies a few 10's of Kev) appearing on L shells of 3 or 4 (Frank, 1967). This current develops first in the afternoon-evening sector of the magnetosphere (Cahill, 1966) and is probably related to the simultaneous occurrence of magnetospheric substorms (Akasofu and Chapman, 1963; Davis and Parthasarathy, 1967). Magnetic effects of the ring current create a depression of the field strength observed on the ground and at the location of the particles. The magnetic field becomes inflated since dipole lines which would normally cross the equatorial plane near the earth are forced further out into the magnetosphere.

This addition of field lines to the outer magnetosphere will result in either (1) extending the magnetopause and keeping the field strength constant, (2) increasing the field strength and keeping the magnetopause position constant, (3) causing a readjustment in the magnetosphere

configuration so that additional lines of force go into the geomagnetic tail, or (4) a combination of these 3 alternatives. No clear evidence exists for movement of the magnetopause boundary during periods of high Kp (Patel and Dessler, 1966) but there are observations of unusually distant boundary crossings during the recovery phase of storms (Cahill and Patel, 1967).

Evidence does exist for additional lines of force moving to the geomagnetic tail during storms. Behannon and Ness (1966) demonstrated that the field of the tail tended to increase during periods of high Kp. Figure 11 from Behannon and Ness shows the IMP 1 measurements of the magnitude F, latitude angle  $\theta$  and longitude angle  $\phi$  in the tail during a three day storm period in May, 1964. The tail field increases abruptly at the time of the storm sudden commencement at 0035 UT on May 10 and tends to remain high until the spacecraft approaches the neutral sheet near the end of May 10. These authors use a tail boundary crossing abnormally close to the X axis and flux conservation arguments to show that only part of the enhanced tail magnitude is due to compression of the tail with the remainder being explained by the addition of lines of force to the tail. Sugiura, et al. (1968) have used precise knowledge of the arrival time of the interplanetary shock associated with the sudden commencement of July 8, 1966 to argue that an observed increase in the tail field at OGO-A was due to additional field lines moving into the tail.

Williams and Ness (1966), Ness and Williams (1966) have used simultaneous measurements of the trapping boundary for electrons  $>280$  kev measured on the low altitude polar orbiting satellite 1963 38C and the IMP 1 magnetic field measurements in the tail to gain further evidence that field lines are added to the tail during magnetic storms.



Figure 12 from Williams and Ness shows three-hour averages of the tail magnetic field along with the high latitude cutoff,  $\Lambda_c$ , and the geomagnetic activity index Kp for two days in April. The circles represent the observed low altitude cutoff for passes of 1963 38C over the polar cap. Open and solid circles designate alternative definitions of the cutoff point. The solid line for  $\Lambda_c$  is obtained by inserting the observed tail field magnitude into the Williams-Mead model of the magnetic field (Williams and Mead, 1965) and noting the latitude of the outermost field lines which could support trapped particles. A sudden commencement storm at 1525 hours on April 1 is reflected in increased values of F and Kp. The observed particle cutoff exhibits a characteristic decrease from pre-storm values of  $66^\circ$  to post SC values near  $60^\circ$ . The value of  $\Lambda_c$  predicted from the field observations undergoes a similar change in latitude even though the absolute values are higher. The difference in absolute value is attributed primarily to inadequacies of the model and the observed changes are attributed to the addition of field lines to the tail. The lower fields and larger differences between the two methods on April 2 are due to IMP 1 measuring the weak fields associated with the equatorial region.

## 2. Effects of Substorms

Information on the behavior of the magnetospheric magnetic fields during substorms has been obtained from the OGO-A and ATS spacecraft. Figure 12 (Heppner, et al., 1967) shows 33 hours of data from an inbound pass of OGO-A through the tail region. The top portion shows the XY component of the tail field and the Z component while the lower portion of the figure shows two auroral zone magnetograms along with

Kp. Changes in field magnitude at 1937 and 2139 in the tail are seen to be associated with magnetic bays observed on the ground near the longitude of the spacecraft. The ground perturbations have earlier onset times of 1922 and 2125. Decreases in the field magnitude at the time of a bay occur when the spacecraft is in a region where the field is greater than that predicted by spherical harmonic reference fields. If the spacecraft is in the region near the equatorial plane between 6 and 11  $R_E$  where the field is normally below the reference field, the spacecraft sees an increase at the time of a bay. In either case the tendency is for the field to evolve toward a more dipole-like configuration following the bay. (see also Sugiura, et al., 1968).

Data from the ATS satellite in a synchronous orbit at 6.6  $R_E$  have yielded additional significant results on the behavior of the magnetospheric magnetic field during substorms (Cummings and Coleman, 1968a; Cummings, et al., 1968). The most prominent feature in the ATS data is a tendency for the field magnitude to be depressed in the dusk-midnight quadrant during disturbed periods as is illustrated in Figure 14 (Cummings, et al., 1968). This depression in H at ATS (0400-1000 UT = 1800-2400 LT) is typically accompanied by a very similar depression on the Honolulu H magnetogram (bottom trace Figure 14) near the sub satellite point and a +H perturbation at College which is located near the foot of the ATS field line. The expansive phase of a substorm then corresponds to a recovery of the field at ATS in a manner similar to that described by Heppner, et al., 1967. This recovery can be seen near 1000 UT (local midnight) in Figure 14 and is accompanied by a very similar change at Honolulu. The striking correspondence between

the observations at ATS and Honolulu refutes the traditional interpretation that bay effects observed on mid-latitude surface magnetograms are due to return currents from the auroral electrojet which flow only in the ionosphere between the ground and the spacecraft. An explanation now seems to require partial ring currents flowing down field lines and closing through the ionosphere (Cummings, et al., 1968; Meng and Akasofu, 1968; Schield, et al., 1969).

The plasma and energetic particle detectors on the Vela spacecraft have yielded data which is relevant to the question of the magnetic field configuration (Hones, et al., 1967; Hones and Singer, 1968). These workers find that if a Vela spacecraft is in the plasma sheet at the time a bay develops, the electrons are decreased in energy or tend to disappear. At the peak of the bay or during the recovery of the bay, the plasma and electrons reappear. Even when a spacecraft is several earth radii from the position of the plasma sheet the electrons and plasma tend to be seen during the recovery of the bay. The authors interpret their results as indicating that substorms originate within the orbit of Vela and only during the recovery do plasma and particles reach the tail.

Rothwell and Wallington (1968) use measurements from the IMP 2 spacecraft with a more eccentric orbit to verify and extend the results of Hones, et al. Rothwell and Wallington find that electron intensities in the outer magnetosphere between 5 and 9  $R_E$  increase simultaneously with auroral zone bays while the electrons appearing beyond these distances are seen after the bays and with greater time delays at greater distances. The authors suggest the Kennel-Petchev (1966) mechanism

is instrumental in the deflation of tubes of force. This region would propagate outward with the magnetoacoustic velocity which could explain the observed delay times.

Rao (1969) has investigated Injun 4 data to determine the effects of substorms on the low altitude outer trapping boundary of  $>40$  kev electrons, which usually is located between  $64^{\circ}$  and  $69^{\circ}$  invariant latitude. He finds that during the expansive phase of a substorm the intensity of the electrons increases but the cutoff latitude tends to remain constant. During the recovery phase of the substorm, however, the cutoff latitude typically moves up to  $75^{\circ}$ . Lin, et al., (1968) observe similar high latitude boundaries during substorms on Alouette 1 and find a corresponding northward movement in the riometer absorption. Although Injun 4 particles are not all trapped, it is probably necessary to have closed field lines up near  $75^{\circ}$  at these times. This situation clearly represents a magnetosphere configuration grossly different from the average picture represented in Figures 2 and 5.

The common feature of all these measurements during substorms is that they point to the existence of a more dipolar-like magnetospheric configuration immediately after a substorm with significantly more flux crossing the equatorial plane near the earth. This relaxed configuration of the magnetosphere after substorms appears to favor theories which suggest storage of the energy for a substorm in the tail (Axford, 1965; Siscoe and Cummings, 1969) but the work of Hones, et al. and Heppner, et al. seems to indicate that the initial effects of the storm take place nearer the earth and not in the tail.

#### IV. Indirect Configuration Measurements

The question of whether the magnetic tail lines of force eventually connect across the neutral sheet or connect with the interplanetary field is of considerable interest. Energetic particles from the sun may provide the best answers to this question. The suggestion is that energetic solar particles will either (1) tend to follow field lines and gain access to the magnetic tail and polar cap almost instantaneously if tail field lines connect to the interplanetary field (the open model), or (2) take many hours to diffuse slowly across the field lines if they are not allowed immediate access. To distinguish between these hypotheses simultaneous particle measurements are required from one spacecraft in the tail or over the polar cap and a second spacecraft measuring ambient flux in the interplanetary medium. The time delay between a change in the ambient flux and the corresponding change observed in the tail or over the polar cap is the relevant quantity to be measured.

Williams and Bostrom (1967) found differences in the interplanetary proton flux at Mariner 4 and the flux averages for passes over the polar cap by Injun 4 and 1963 38C. They attributed these to a changing magnetosphere configuration which alternately improved or detracted from access to the polar cap. Krimigis, et al. (1967) found good agreement between the fluxes observed at Explorer 33 and Injun 4 over the polar cap with a delay less than  $\frac{1}{2}$  hour. These authors interpreted their results as supporting the open model unless diffusion were much more rapid than that predicted by simple particle diffusion theory.

Blake, et al. (1968) studied protons over the polar cap and found higher fluxes at lower latitudes nearer the cutoff point. They warn

against using polar cap averages and feel their results argue against interplanetary connection. Lanzerotti (1968) compares Explorer 34 interplanetary data with ATS data and finds that solar protons have quick access to  $6.6 R_E$ . He suggests that if particles can diffuse to  $6.6 R_E$  so readily, little can be learned about magnetosphere topology from low energy particles. Williams and Bostrom (1969) suggest that the particles have easy access to the neutral sheet and therefore, it is not surprising that they can diffuse rapidly to  $6.6 R_E$ .

The best data pertinent to this question of access to the tail are the recent data of Montgomery, et al. (1969). These authors consider simultaneous Vela measurements which clearly show that flux changes in the tail are delayed by times ranging from 15 minutes to 2 hours. Often sharp flux increases outside the tail were broadened in the tail but the delays were not energy dependent. The fluxes were often anisotropic outside and away from the tail and isotropic near and within the tail. These measurements fail to support the open magnetosphere model in that a time delay is observed and the particles are not anisotropic. The measurements also fail to support diffusion theory in that the delay is not as long as predicted and no energy dependence is found. After considering these results which do not fully support either theory, the authors suggest an intermediate interpretation of multiple scattering in and near the tail with merging of tail and interplanetary fields downstream.

Williams and Bostrom (1969) have compared proton intensities from individual passes of 1963 38C over the polar cap with IMP-4 measurements in the interplanetary medium. They often find enhanced fluxes of

1.2-8.5 Mev protons near the auroral regions following increases in the interplanetary proton fluxes. They interpret these observations as indicating diffusion into each bundle of polar flux. At other times they find polar cap profiles which may be consistent with direct access to the polar cap (Williams, personal communication). Their suggestion is that both means of entry are possible at different times with the exact method depending on the boundary conditions imposed on the magnetosphere by the interplanetary medium.

Less data is available on the entry of electrons to the tail and polar cap. Early measurement by Lin and Anderson suggested that the delay time between a solar flare and the observations of the associated electrons was not strongly dependent on whether or not the spacecraft was in the tail. This observation was cited as favoring the open magnetosphere model, but if diffusion is at all important this would not be so. Van Allen and Ness (1968) use particle shadowing by the moon to demonstrate that the diffusion velocity of solar electrons across the tail is less than  $100 \text{ km sec}^{-1}$ . Lin (1968) uses similar particle measurements near the moon and concludes that the electrons have direct access to the tail beyond the orbit of the moon.

The net result of all these particle measurements is that they have been unable to supply definitive information on whether field lines in the tail connect to those of interplanetary space. Diffusion appears to play a role in the entry of particles to the tail but it appears to be much more rapid than previously predicted (Michel and Dessler, (1965)). Direct access along field lines connecting directly to the interplanetary medium may also occur at certain times.

Connection of magnetosphere field lines to those of the interplanetary medium may be tested directly by studying magnetopause crossings and searching for a field component normal to the boundary. Sonnerup and Cahill (1967) studied Explorer 12 data and concluded that sometimes there was evidence for such connection. Cummings and Coleman (1968b) studied rare boundary crossings at the  $6.6 R_E$  synchronous distance and concluded there was no connection.

Fairfield and Cahill (1966) have shown that geomagnetic activity tends to be higher when the magnetosheath field has a southward component. Since a southward interplanetary field should correspond to the greatest connection, the most rapid magnetosphere convection, and the highest geomagnetic activity, this result has been interpreted as indirect evidence for the connection of the interplanetary field to that of the magnetosphere. This experimental evidence associating a southward field with geomagnetic activity has been well verified (see review by Hirshberg and Colburn, 1968) but an alternate interpretation of the results is still a possibility.



## V. Summary and Conclusions

Mid-latitude dipole field lines are simultaneously compressed by the solar wind in the sunlit hemisphere, extended in the night hemisphere and distorted from the meridian planes. High latitude field lines are swept back to form the geomagnetic tail. The outermost closed field line originates near  $78^\circ$  on the day side of the earth and near  $68^\circ$  on the night side. Lines from the south polar cap directed away from the earth form the lower half of the geomagnetic tail while lines from the north polar cap directed toward the earth form the upper half of the tail. These two halves are separated by a neutral sheet less than  $1 R_E$  thick which is itself contained within a broad region of depressed fields approximately  $12 R_E$  thick. The average magnitude of the tail field decreases from a value of  $20\gamma$  at  $15 R_E$  to a value of  $8\gamma$  at  $60 R_E$ . Any magnitude gradient beyond  $60 R_E$  is very small. The cross-section of the tail is elliptical with typical transverse dimensions of  $45 R_E$  east-west and  $60 R_E$  north-south at the orbit of the moon. The average tail-field direction makes a small angle with the earth-sun line which is consistent with the aberration associated with the earth's motion about the sun. The magnetic tail has been observed for brief intervals (minutes to hours) at  $500 R_E$  and  $1000 R_E$ . These observations are interpreted as being caused by either filamentary structure of the tail or by rapid movement of the tail past the spacecraft in response to changing solar wind directions.

Important changes in the magnetospheric magnetic field configuration occur at the time of magnetic storms and substorms. The ring current associated with main phase magnetic storms inflates the inner magnetosphere forcing the equatorial crossing point of field lines out further into the magnetosphere. At the same time the outer boundary of trapped particles collapses and the field strength in the tail increases. These results are interpreted as an increase in the number of field lines forming the tail.

Magnetospheric substorms correspond to a relaxation of the magnetosphere towards a more dipolar-like state with more lines of force closing near the earth. This relaxation is suggested by direct measurements of the magnetic field and supported by the observed increase in the trapped particle boundary to  $75^\circ$  after substorms. The appearance of plasma and particles at  $17 R_E$  after substorms is further evidence supporting this relaxation. The fact that magnetospheric substorms cause gross readjustments in the magnetosphere configuration should be taken into consideration when using an average magnetosphere configuration. Roederer, et al. (1968) have partially circumvented the problem of time variations by using the measurements of a synchronous satellite as input to a field model which defines the field at all points.

The question of connection of the magnetosphere lines of force to the interplanetary lines has not been fully resolved. Access of

energetic particles to the tail and polar cap appears to be easier than that expected for diffusion but lower than that expected for direct access. The experimental evidence relating the interplanetary field to geomagnetic activity has been confirmed. This result has been interpreted as evidence for connection; however, another interpretation is possible.

## VI. Future Work

The general properties of a time averaged magnetosphere are rather well known. Numerous spacecraft have probed the outer magnetosphere in latitudes below  $60^\circ$  but the higher latitude regions are still unexplored. Although Figure 1 does not reveal any obvious dawn-dusk asymmetry, the ATS measurements suggest that such effects do exist. This question can be studied in the future with additional equatorial measurements in the dusk hemisphere.

The most important magnetosphere problems lie in the area of time variations. Adjustments in the field configuration at the time of magnetic storms and substorms have recently been investigated but additional work is called for. Field changes must be studied as a function of local time and related to changes in the magnetospheric plasma and particles. Further studies of trapped particles are needed to give information on the latitude of the outermost closed field lines near midnight and how they vary with time.

Detailed studies are needed to determine whether the magnetopause is (1) a tangential discontinuity indicating complete separation of geomagnetic and interplanetary field lines, (2) a rotational discontinuity with geomagnetic field lines connecting to the interplanetary field, or (3) tangential and rotational discontinuities at different times. The above investigation is relevant to the very important questions of how field lines are dragged back to form the tail and how energy is transferred from the solar wind to the magnetosphere.

The exact nature of the tail at 500-1000  $R_E$  and its extent beyond 1000  $R_E$  remain unanswered questions. Finally the development of improved quantitative models of the magnetosphere and tail which include time variations should be a future goal.

Acknowledgements

The author would like to thank Mr. K. W. Behannon and Drs. N. F. Ness, D. J. Williams and F. Mariani for helpful discussions and access to their data prior to publication.

## REFERENCES

- Akasofu, S. I. and S. Chapman, Magnetic Storms: The Simultaneous Development of the Main Phase (DR) and of Polar Magnetic Substorms (DP), J. Geophys. Res., 68, 3155-3158, 1963.
- Axford, W. I., Magnetic Storm Effects Associated with the Tail of the Magnetosphere, paper presented at ESRO Conference on the Magnetosphere, November 1965.
- Bame, S. J., J. R. Asbridge, H. E. Felthausen, E. W. Hones and I. B. Strong, Characteristics of the Plasma Sheet in the Earth's Magnetotail, J. Geophys. Res., 72, 113-129, 1967.
- Behannon, Kenneth W., Mapping of the Earth's Bow Shock and Magnetic Tail by Explorer 33, J. Geophys. Res., 73, 907-930, 1968.
- Behannon, Kenneth W., Geometry of the Geomagnetic Tail, Goddard Space Flight Center preprint, April 1969.
- Behannon, K. W. and N. F. Ness, Magnetic Storms in the Earth's Magnetic Tail, J. Geophys. Res., 71, 2327-2351, 1966.
- Blake, J. B., G. A. Paulikas, and S. C. Freden, Latitude-Intensity Structure and Pitch-Angle Distributions of Low-Energy Solar Cosmic Rays at Low Altitude, J. Geophys. Res., 73, 4927-4934, 1968.
- Brandt, John C., Charles Wolff, and Joseph P. Cassinelli, Interplanetary Gas XVI. A calculation of the Angular Momentum of the Solar Wind, preprint, 1969.
- Cahill, Laurence J. Jr., Inflation of the Inner Magnetosphere During a Magnetic Storm, J. Geophys. Res., 71, 4505-4519, 1966.
- Cahill, L. J., Jr. and V. L. Patel, The Boundary of the Geomagnetic Field, August to November 1961. Planet. and Space Sci., 15, 997-1033, 1967.
- Cummings, W. D., and P. J. Coleman, Jr., Simultaneous Magnetic Field Variations at the Earth's Surface and at Synchronous, Equatorial Distance. Part 1, Bay Associated Events, Radio Sci., 3, 758-761, 1968a.

- Cummings, W.D. and P. J. Coleman, Jr., Magnetic Fields in the Magnetopause and Vicinity at Synchronous Altitude, J. Geophys. Res., 73, 5699-5718, 1968b.
- Cummings, W. D., J. N. Barfield and P. J. Coleman, Jr., Magnetosphere Substorms Observed at the Synchronous Orbit, 73, 6687-6698, 1968.
- Davis, T. N. and R. Parthasarathy, The Relationship Between Polar Magnetic Activity DP and Growth of the Geomagnetic Ring Current, J. Geophys. Res., 72, 5825-5836, 1967.
- Dungey, J. W., Theory of the Quiet Magnetosphere, in "Solar Terrestrial Physics", (J. W. King and W. S. Newman, eds.), p. 91-106, Academic Press, New York, 1968.
- Fairfield, D. H., and L. J. Cahill, Jr., Transition Region Magnetic Field and Polar Magnetic Disturbances, J. Geophys. Res., 71, 155-169, 1966.
- Fairfield, D. H., Average Magnetic Field Configuration of the Outer Magnetosphere, J. Geophys. Res., 73, 7329-7338, 1968a.
- Fairfield, D. H., Simultaneous Measurements on Three Satellites and the Observation of the Geomagnetic Tail at 1000  $R_E$ , J. Geophys. Res., 73, 6179-6187, 1968b.
- Feldstein, Y. I. Some Problems Concerning the Morphology of Auroras and Magnetic Disturbances in High Latitudes, Geomag. and Aeronomy 3, 183-192, 1963.
- Frank, L. A., J. A. Van Allen and J. D. Craven, Large Diurnal Variations of Geomagnetically Trapped and of Precipitated Electrons Observed at Low Altitudes, J. Geophys. Res., 69, 3155-3167, 1964.
- Frank, L. A., On the Extraterrestrial Ring Current During Geomagnetic Storms, J. Geophys. Res., 72, 3753-3767, 1967.
- Heppner, J. P., M. Sugiura, T. L. Skillman, B. G. Ledley, and M. Campbell, OGO-A Magnetic Field Observations, J. Geophys. Res., 72, 5417-5471, 1967.
- Hirshberg, J. and D. S. Colburn, Interplanetary Field and Geomagnetic Variations - A Unified View, to be published Planet and Space Sci. 1969.
- Hones, E. W. Jr., J. R. Ashbridge, S. J. Bame and I. B. Strong, Outward Flow of Plasma in the Magnetotail Following Geomagnetic Bays, J. Geophys. Res., 72, 5879-5892, 1967.



- Hones, E. W., Jr. and S. Singer, Simultaneous Observations of Electrons ( $E > 45$  kev) at 2000 Kilometer Altitude and at 100,000 Kilometers in the Magnetotail, J. Geophys. Res., 73, 7339-7359, 1968.
- Kennel, C. F. and H. E. Petschek, Limit on Stably Trapped Particle Fluxes, J. Geophys. Res., 71, 1-28, 1966.
- Krimigis, S. M., J. A. Van Allen and T. P. Armstrong, Simultaneous Observations of Solar Protons Inside and Outside the Magnetosphere, Phys. Rev. Letters, 18, 1204-1206, 1967.
- Lanzerotti, L. J., Penetration of Solar Protons and Alphas to the Geomagnetic Equator, Phys. Rev. Letters, 21, 929-933, 1968
- Lin, R. P. Observations of Lunar Shadowing of Energetic Particles, J. Geophys. Res., 73, 3066-3071, 1968.
- Lin, R. P., and K. A. Anderson, Evidence for Connection of Geomagnetic Tail Lines to the Interplanetary Field, J. Geophys. Res., 71, 4213-4217, 1966.
- Lin, W. C. I. B. McDiarmid and J. R. Burrows, Electron Fluxes at 1000 Km Altitude Associated with Auroral Substorms, Can. J. Phys. 46, 80-83, 1968.
- Mariani, F. and N. F. Ness, Observation of a Filamentary Geomagnetic Tail at 500 Earth Radii by Pioneer 8, Goddard Space Flight Center preprint X616-69-54, 1969.
- Mead, G. D. Deformation of the Geomagnetic Field by the Solar Wind, J. Geophys. Res., 69, 1181-1195, 1964.
- Meng, C. I. and S. I. Akasofu, A Study of Polar Magnetic Substorms-II Three Dimensional Current System, Preprint, Geophysical Institute of the University of Alaska 1969.
- Michel, F. C. and A. J. Dessler, Physical Significance of Inhomogenities in Polar Cap Absorption Events, J. Geophys. Res., 70, 4305-4311, 1965.
- Mihalov, J. D., D. S. Colburn, R. G. Currie and C. P. Sonett, Configuration and Reconnection of the Geomagnetic Tail, J. Geophys. Res., 73, 943-959, 1968.
- Montgomery, Michael, D. and S. Singer, Penetration of Solar Energetic Protons Into the Magnetotail, U. of Cal., Los Alamos Scientific Laboratory preprint No. LA-DC-9271.
- Ness, N. F., The Earth's Magnetic Tail, J. Geophys. Res., 70, 2989-3005, 1965.

- Ness, Norman F., The Geomagnetic Tail, Reviews of Geophysics, 7, February 1969.
- Ness, N. F., K. W. Behannon, S. C. Cantarano and C. S. Scearce, Observations of the Earth's Magnetic Tail and Neutral Sheet at 510,000 Kilometers by Explorer 33, J. Geophys. Res., 72, 927-933, 1967a.
- Ness, Norman F., Clell S. Scearce and Sergio C. Cantarano, Probable Observations of the Geomagnetic Tail at  $10^3 R_E$  by Pioneer 7, J. Geophys. Res., 72, 3769-3776, 1967b.
- Ness, N. F. and Williams, D. J., Correlated Magnetic Tail and Radiation Belt Observations, J. Geophys. Res., 71, 322-325, 1966.
- Patel, V. L. and A. J. Dessler, Geomagnetic Activity and Size of Magnetospheric Cavity, J. Geophys. Res., 71, 1940-1942, 1966.
- Rao, C. S. R., Some Observations of Energetic Electrons in the Outer Radiation Zone During Magnetic Bays, J. Geophys. Res., 74, 794-801, 1969.
- Roederer, Juan G., Warren D. Cummings, Paul J. Coleman and Marilyn F. Robbins, Determination of Magnetospheric Parameters from Magnetic Field Measurements at Synchronous Altitudes, University of Denver Department of Physics, Denver Research Institute Report 1968.
- Rothwell, P. and V. Wallington, The Polar Substorm and Electron 'Islands' in the Earth's Magnetic Tail, Planet. and Space Sci. 16, 1441-1451, 1968.
- Schild, M. A., J. W. Freeman and A. J. Dessler, A Source for Field-Aligned Currents at Auroral Latitudes, J. Geophys. Res., 74, 247-256, 1969.
- Siscoe, G. L. and W. D. Cummings, On the Cause of Geomagnetic Bays, UCLA preprint February 1969.
- Sonnerup, B. U. Ö., and L. J. Cahill, Jr., Magnetopause Structure and Attitude From Explorer 12 Observations, J. Geophys. Res., 72, 171, 183, 1967.
- Speiser, T. W. and N. F. Ness, The Neutral Sheet in the Geomagnetic Tail: Its Motion, Equivalent Currents, and Field Line Reconnection Through It, J. Geophys. Res., 72, 131-141, 1967.

- Sugiura, Masahisa, Results of Magnetic Surveys of the Magnetosphere and Adjacent Regions, Goddard Space Flight Center preprint X612-69-12, January 1969. Presented at the IAGA Symposium on Description of the Earth's Magnetic Field, Washington, D.C., October 1968, to be published in the Report of the World Magnetic Survey.
- Sugiura, M., T. L. Skillman, B. G. Ledley, and J. P. Heppner, Propagation of the Sudden Commencement of July 8, 1966 to the Magnetotail, J. Geophys. Res., 73, 6609-6709, 1968.
- Taylor, Harold E., and Edward W. Hones, Jr., Adiabatic Motion of Auroral Particles in a Model of the Electric and Magnetic Fields Surrounding the Earth, J. Geophys. Res., 3605-3628, 1965.
- Van Allen, J. A. and N. F. Ness, Particle Shadowing by the Moon, J. Geophys. Res., 74, 71-93, 1969.
- Williams, D. J. and C. O. Bostrom, The February 5, 1965 Solar Proton Event 2. Low Energy Proton Observations and Their Relation to the Magnetosphere, J. Geophys. Res., 72, 4490-4506, 1967.
- Williams, D. J. and C. O. Bostom, Proton Entry in the Magnetosphere on May 26, 1967. Goddard Space Flight Center preprint, April 1969.
- Williams, Donald J., and Gilbert D. Mead, Nightside Magnetosphere Configuration as Obtained from Trapped Electrons at 1100 Kilometers, J. Geophys. Res., 70, 3017-3029, 1965.
- Williams, Donald J., and Norman F. Ness, Simultaneous Trapped Electron and Magnetic Tail Field Observations, J. Geophys. Res., 71, 5117-5128, 1966.
- Wolfe, J. H., R. W. Silva, D. D. McKibbin, and R. H. Mason, Preliminary Observations of a Geomagnetic Wake at 1000 Earth Radii, J. Geophys. Res., 72, 4577-4581, 1967.
- Zmuda, A. J., F. T. Heuring and J. H. Martin, Dayside Magnetic Disturbances at 1100 Kilometers in the Auroral Oval, J. Geophys. Res., 72, 1115-1117, 1967.

## FIGURE CAPTIONS

- Figure 1 Southern hemisphere hourly average field vectors projected in the solar magnetic equatorial plane illustrate the sweeping back of field towards the tail by the solar wind. Solid lines denote the average magnetopause and 24 longitudinal sections that have been drawn with the data as a guide (Fairfield, 1968a).
- Figure 2 Contours in the equatorial plane designating the latitude and local time of the earth intersection point of the field line. (Fairfield, 1968a).
- Figure 3 Auroral oval and associated phenomena have been projected along field lines to the equatorial plane using the information of Figure 2 (Fairfield, 1968a).
- Figure 4 Vectors projected in the curved meridian sections of Figure 1 in the 0800-0500 local time regions for hours when the sun is south of the solar magnetic equatorial plane. Solid lines represent distorted field lines which have been drawn with the data and the information of Figure 2 as a guide. Dashed lines represent undistorted dipole field lines corresponding to each distorted line. The lines are labeled with their earth intersection latitudes (Fairfield, 1968a).
- Figure 5 Distorted and dipole lines of the noon-midnight meridian plane. The lines are labeled with their earth intersection latitudes (Fairfield, 1968a).
- Figure 6 Explorer 33 hourly average vectors projected in solar magnetospheric coordinates. The top view shows vectors projected in the noon-midnight meridian plane while the other view shows vectors projected in the equatorial plane when the measurements are taken in the northern hemisphere (middle) and southern hemisphere (bottom). Axes are labeled in earth radii (Behannon, 1968).
- Figure 7 Magnitude of the geomagnetic tail field vs. distance from the tail (Behannon, 1968).
- Figure 8 Magnitude of the tail field vs distance from the solar magnetospheric XY plane. Data show a broad region of depressed fields near  $Z_{SE}=0$ . The RMS values denote the scatter of the hourly averages which were averaged to give the top curve (Behannon, 1969).

- Figure 9 Trajectory intervals when spacecraft observed the magnetotail boundary near the orbit of the moon. The circle is drawn for reference; whereas, the measurements suggest an elliptical cross-section for the tail (Behannon, 1969).
- Figure 10 Intervals of tail like magnetic field observed by Pioneer 7 almost 1000  $R_E$  from the earth. A neutral sheet crossing is seen at 1739 (Ness, 1969).
- Figure 11 Three days of geomagnetic tail data and mid-latitude magnetograms. Enhanced tail magnitudes are seen until the spacecraft approached the weak field region surrounding the neutral sheet on May 11 (Behannon and Ness, 1966).
- Figure 12 Magnetic field parameters, geomagnetic index  $K_p$  and trapped particle cutoff latitude  $\Lambda_c$  for a two day storm period. A decrease in  $\Lambda_c$  after the rise in  $K_p$  is seen in both the direct observations (circles) and the values calculated by putting the observed tail magnitudes in a field model (Williams and Ness, 1966).
- Figure 13 OGO A measurements in the geomagnetic tail illustrating decreases in the tail magnitude which are associated with auroral zone bays observed at earlier times (Heppner et al. 1967).
- Figure 14 ATS measurement of the horizontal field strength  $H$  at the equatorial synchronous orbit are shown along with College and Honolulu magnetograms. A typical depression in  $H$  at ATS and Honolulu in the dusk-midnight quadrant is associated with  $+H$  perturbations at College. Recovery of  $H$  at ATS and Honolulu corresponds to a sharp bay at College (Cummings et al., 1968).

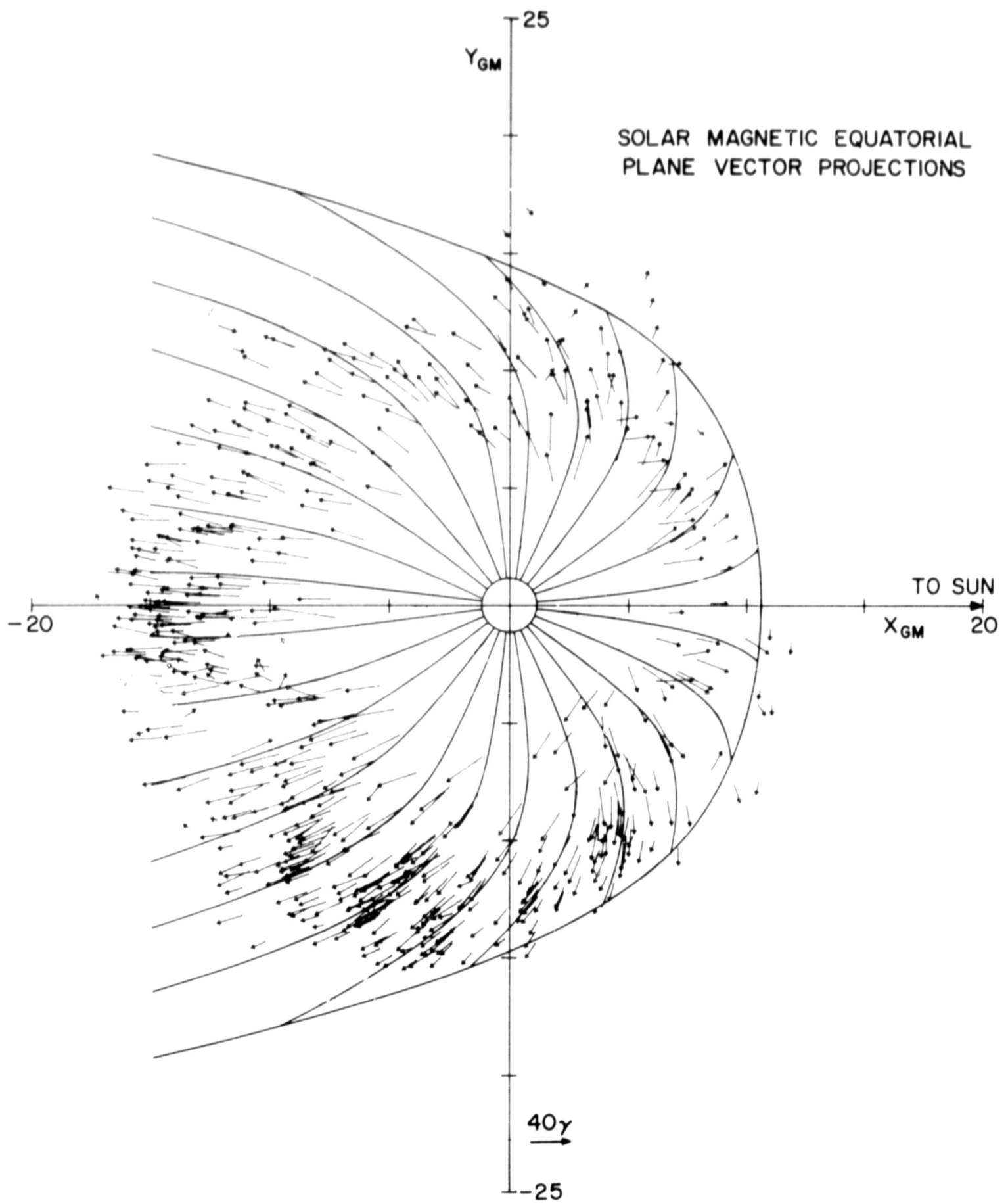


FIGURE 1

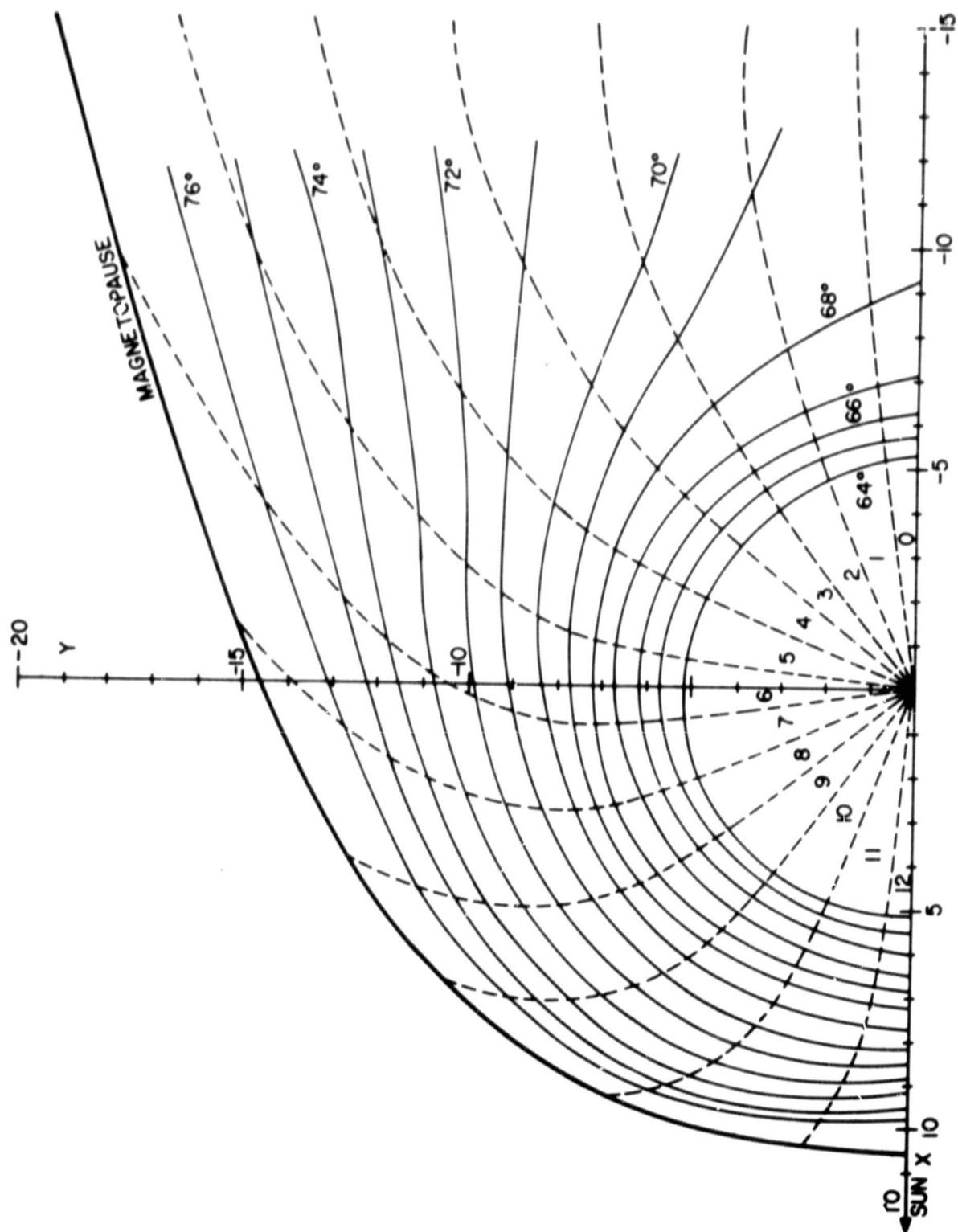


FIGURE 2

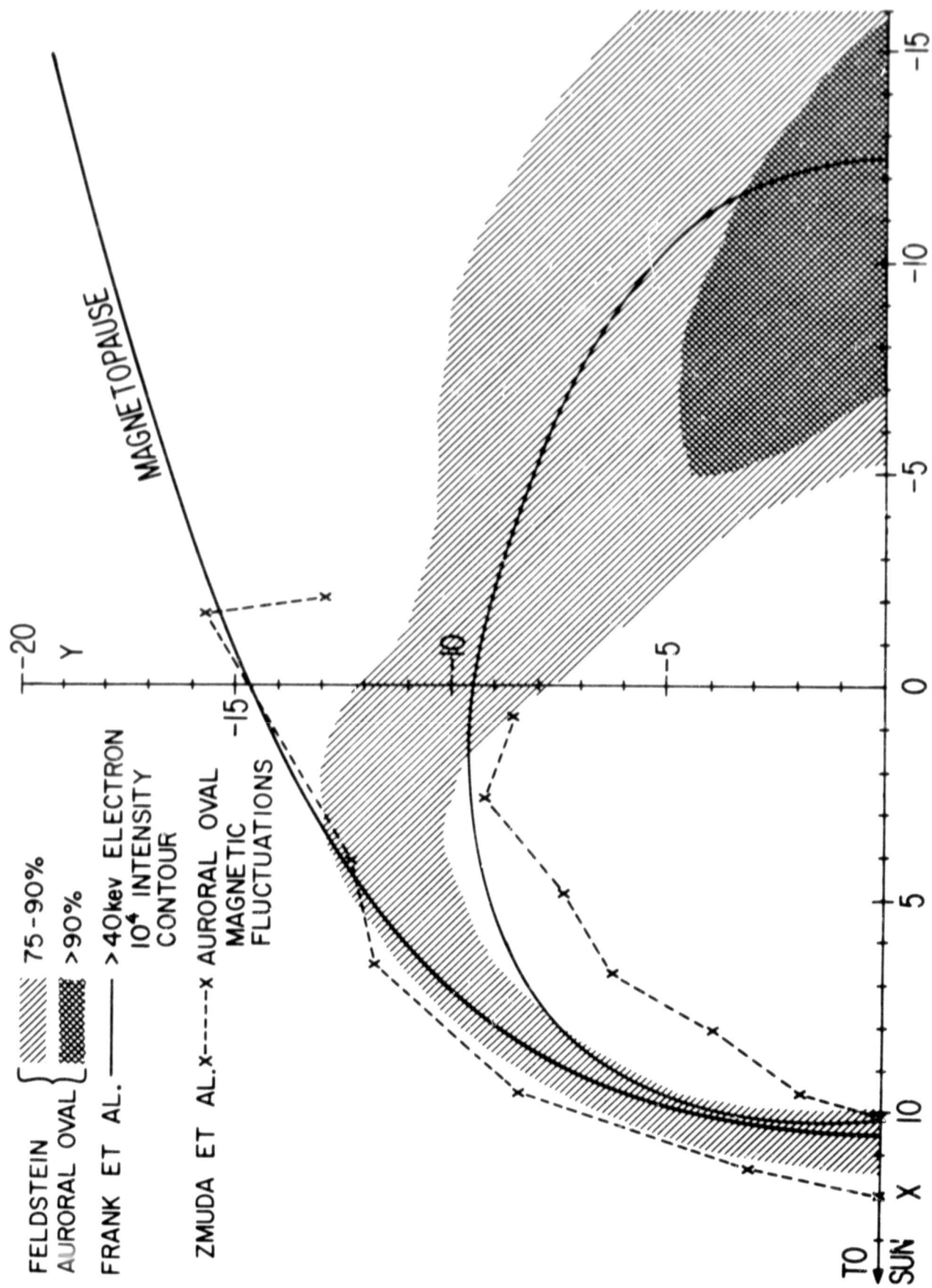


FIGURE 3



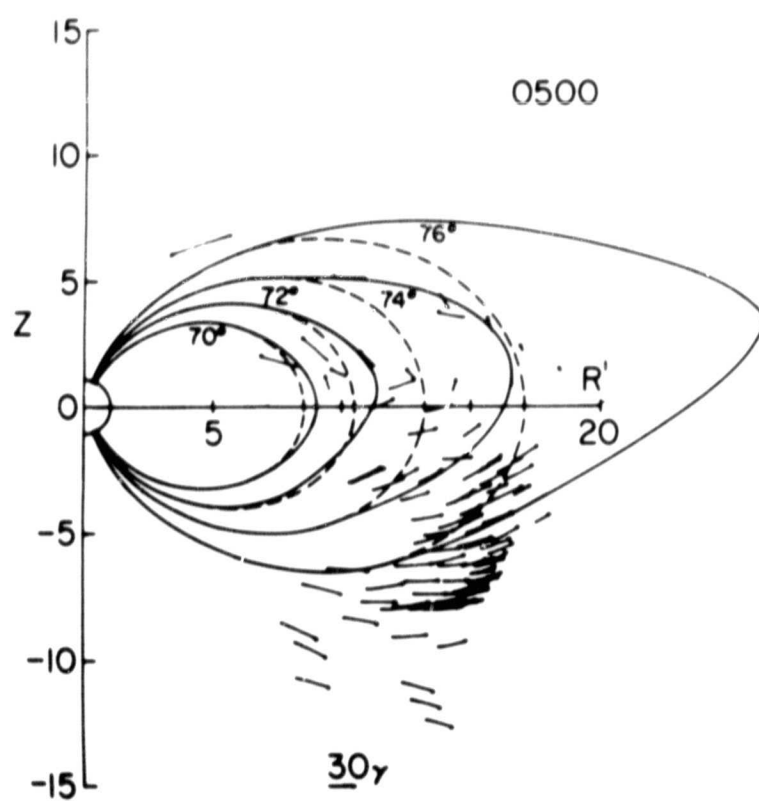
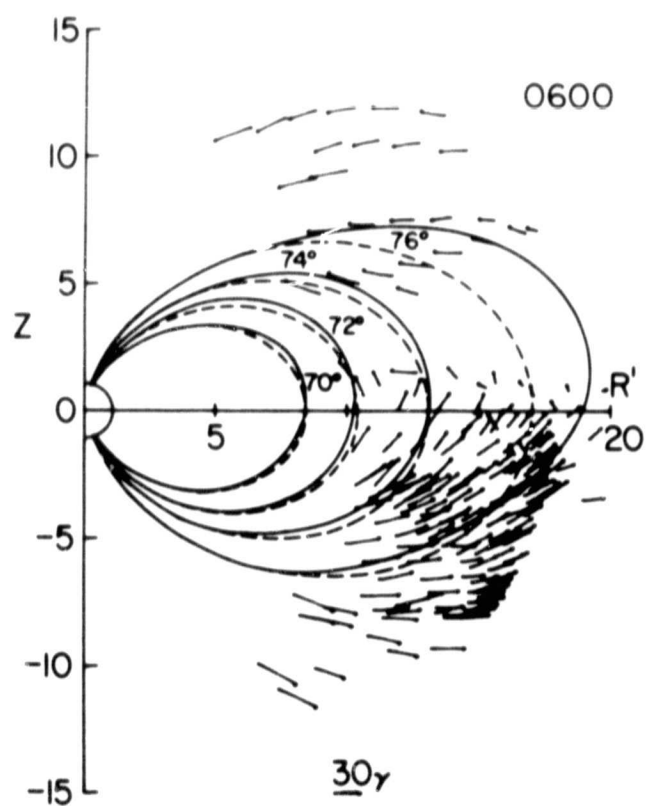
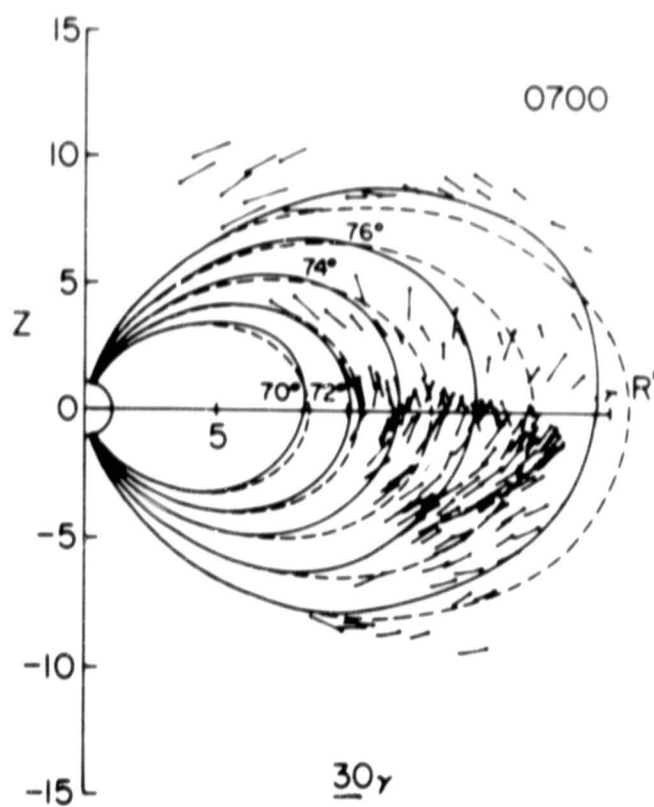
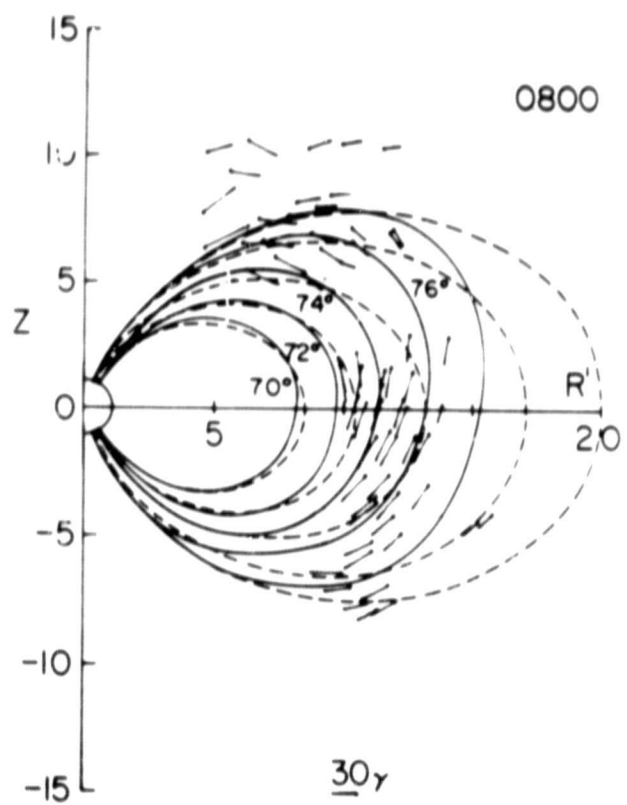


FIGURE 4

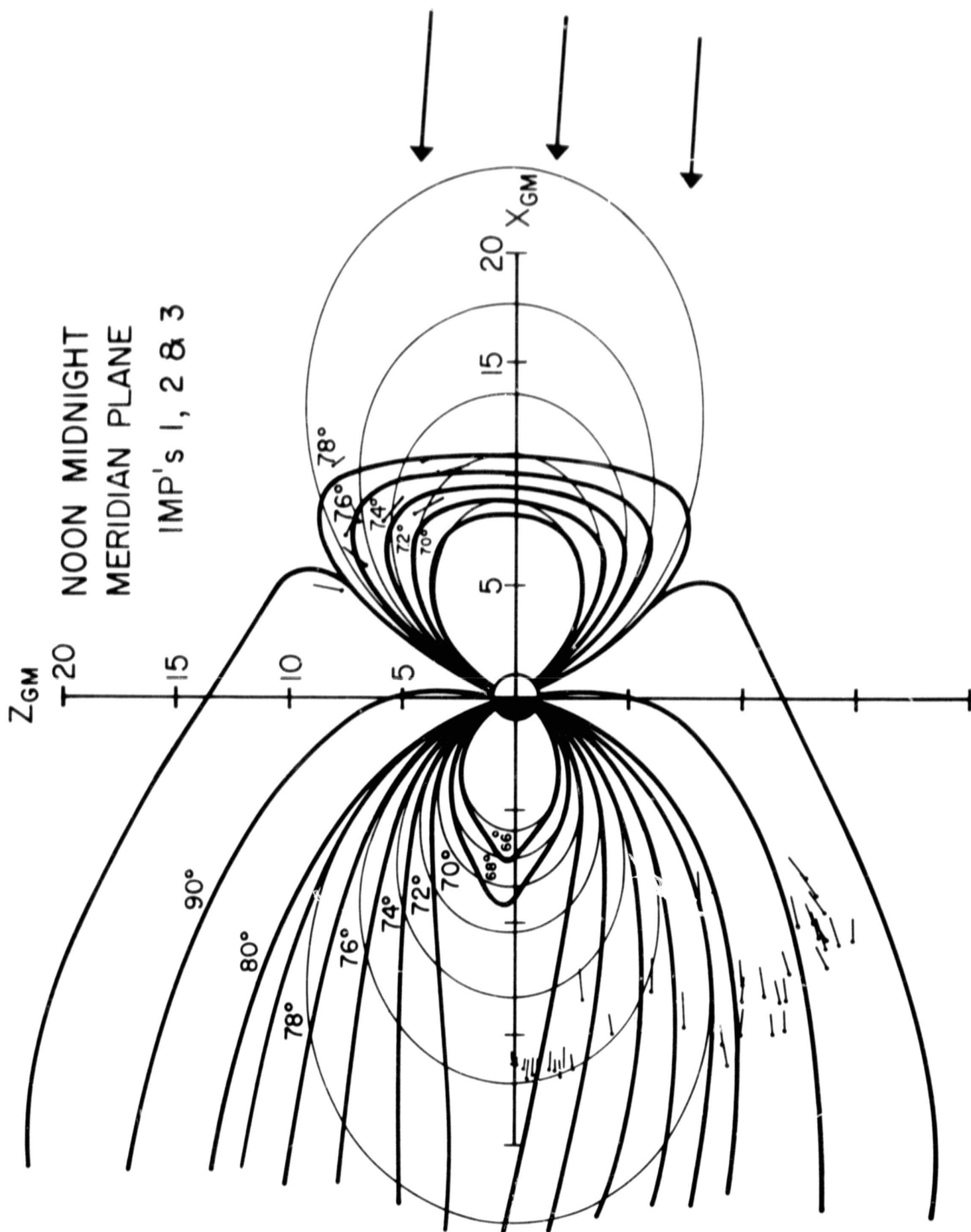


FIGURE 5

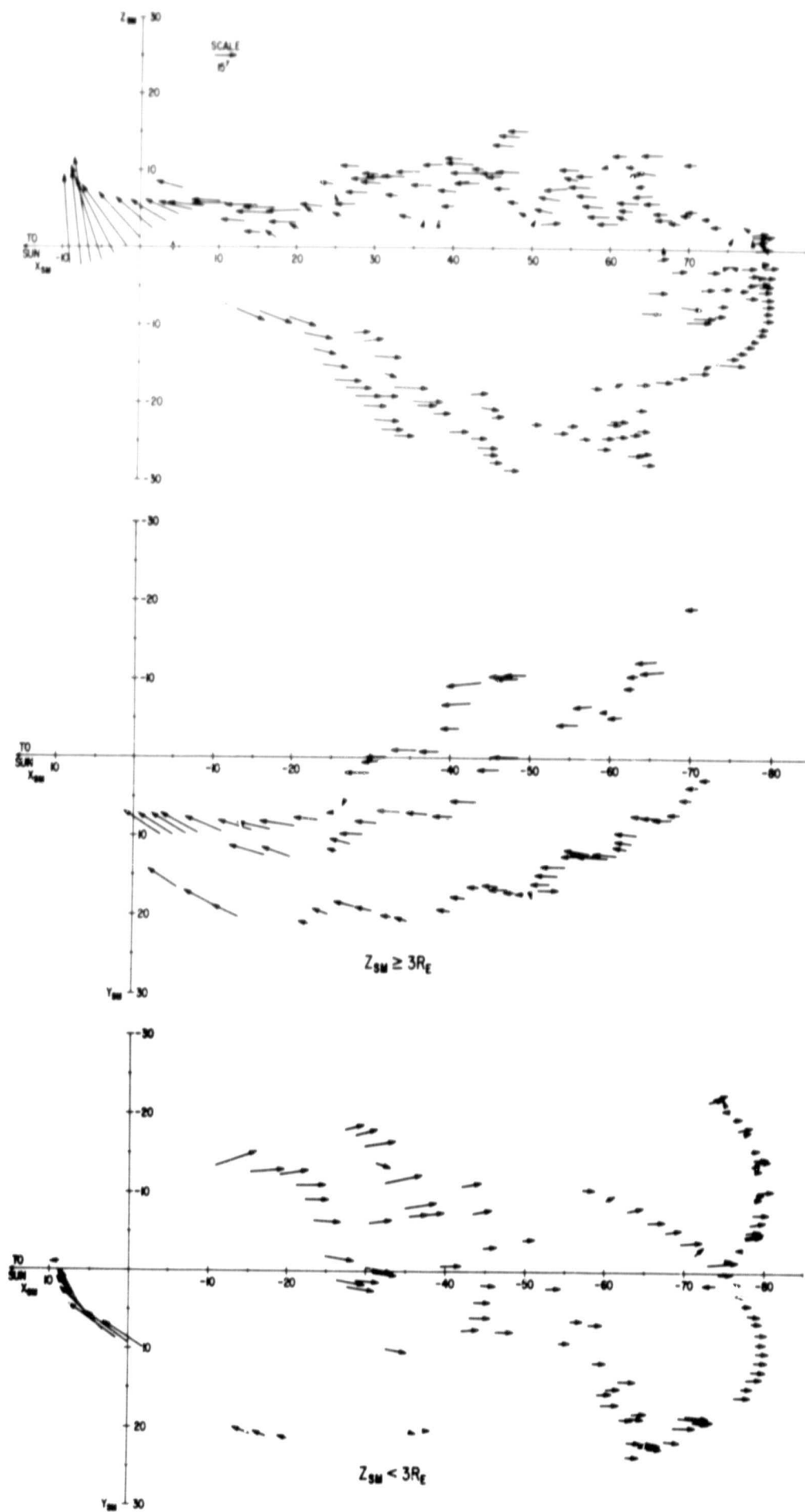


FIGURE 6

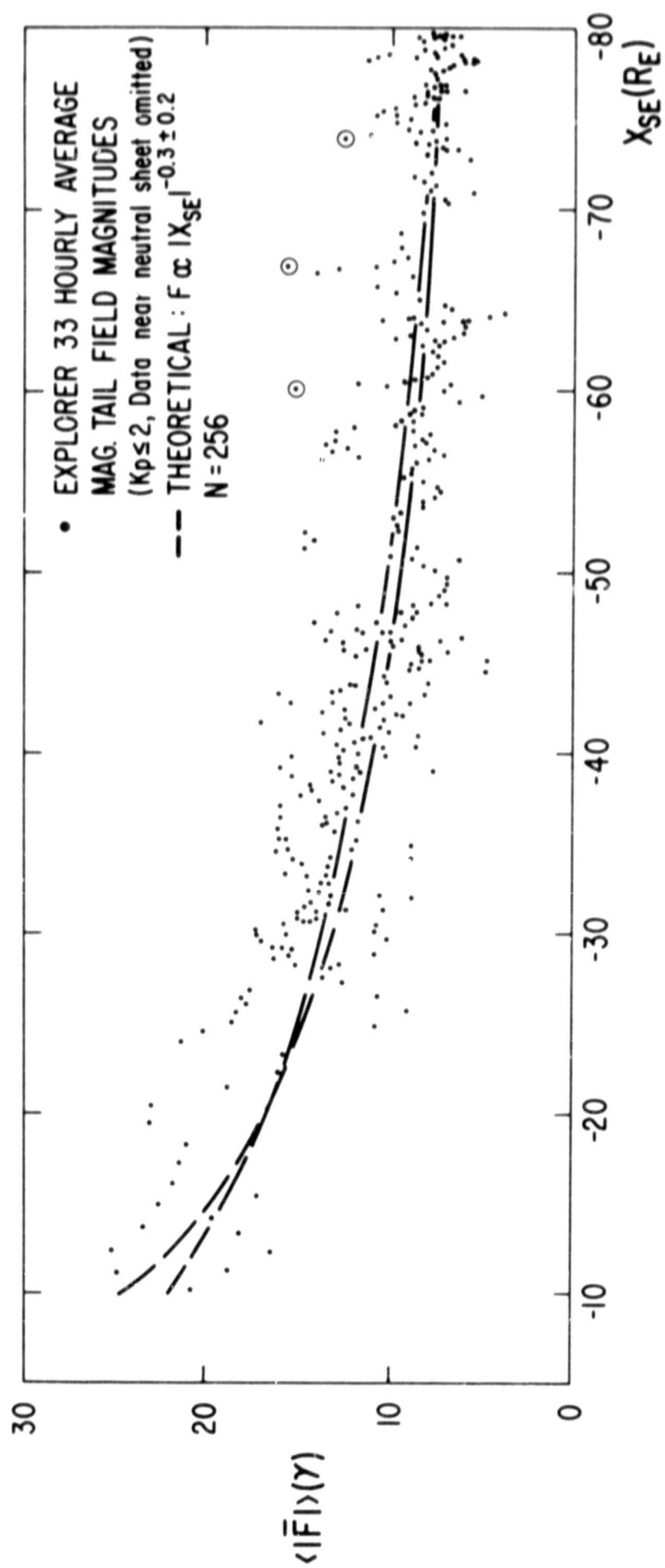


FIGURE 7

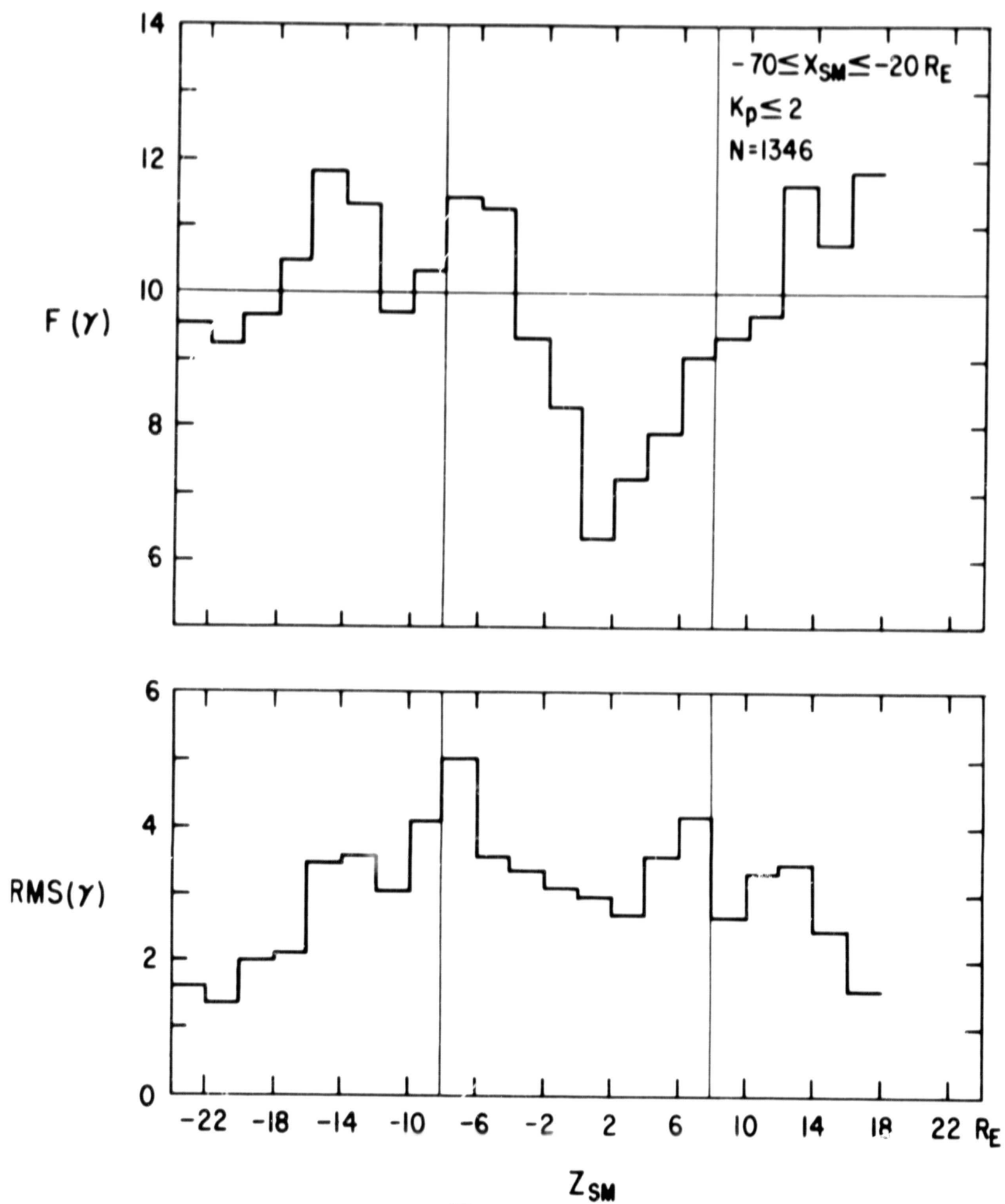
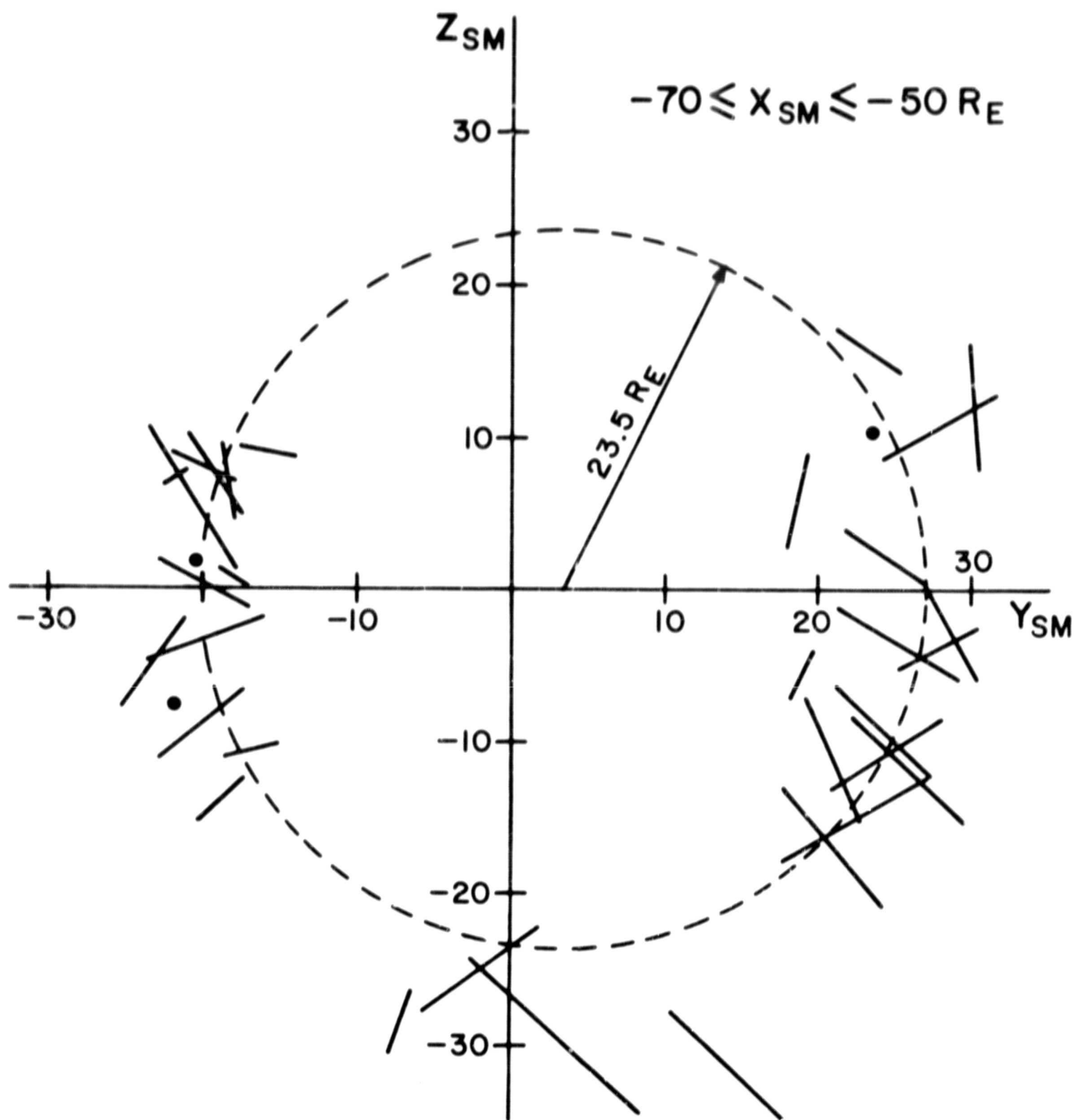
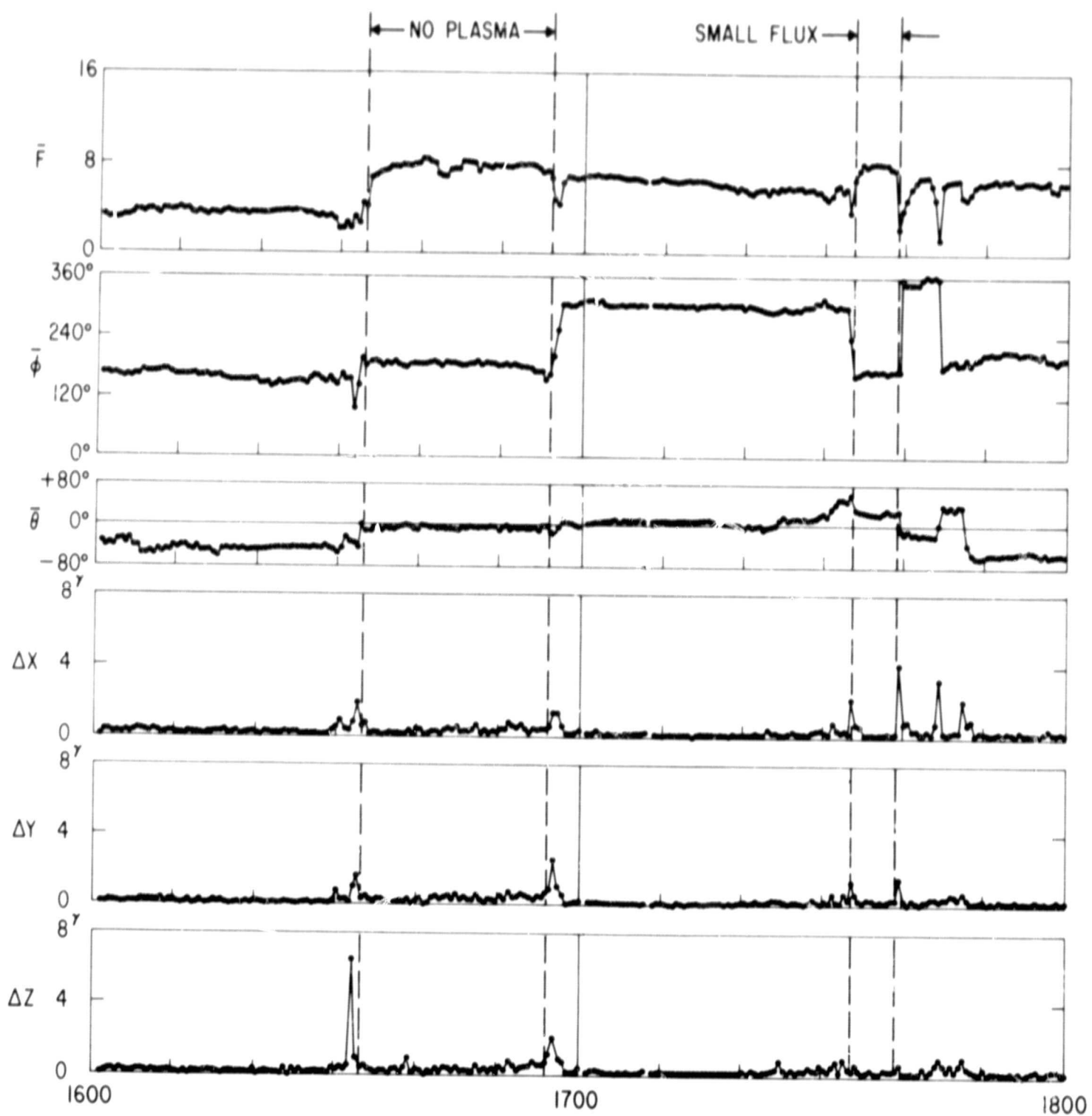


FIGURE 8



MAGNETOTAIL BOUNDARY TRAVERSALS  
EXPLORERS 33 & 35, 1967-68

FIGURE 9



PIONEER 7 SEPT. 26, 1966

FIGURE 10

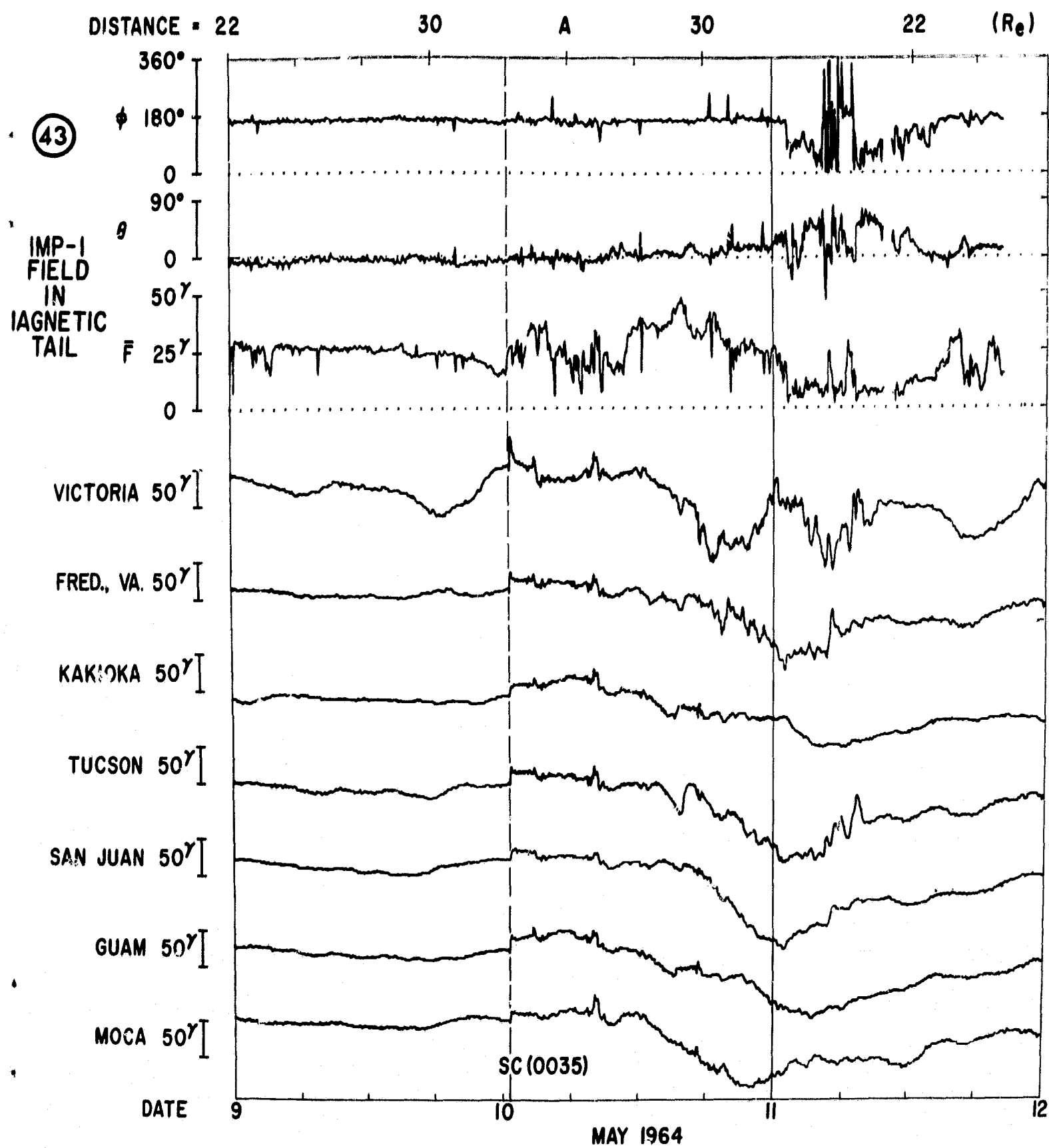
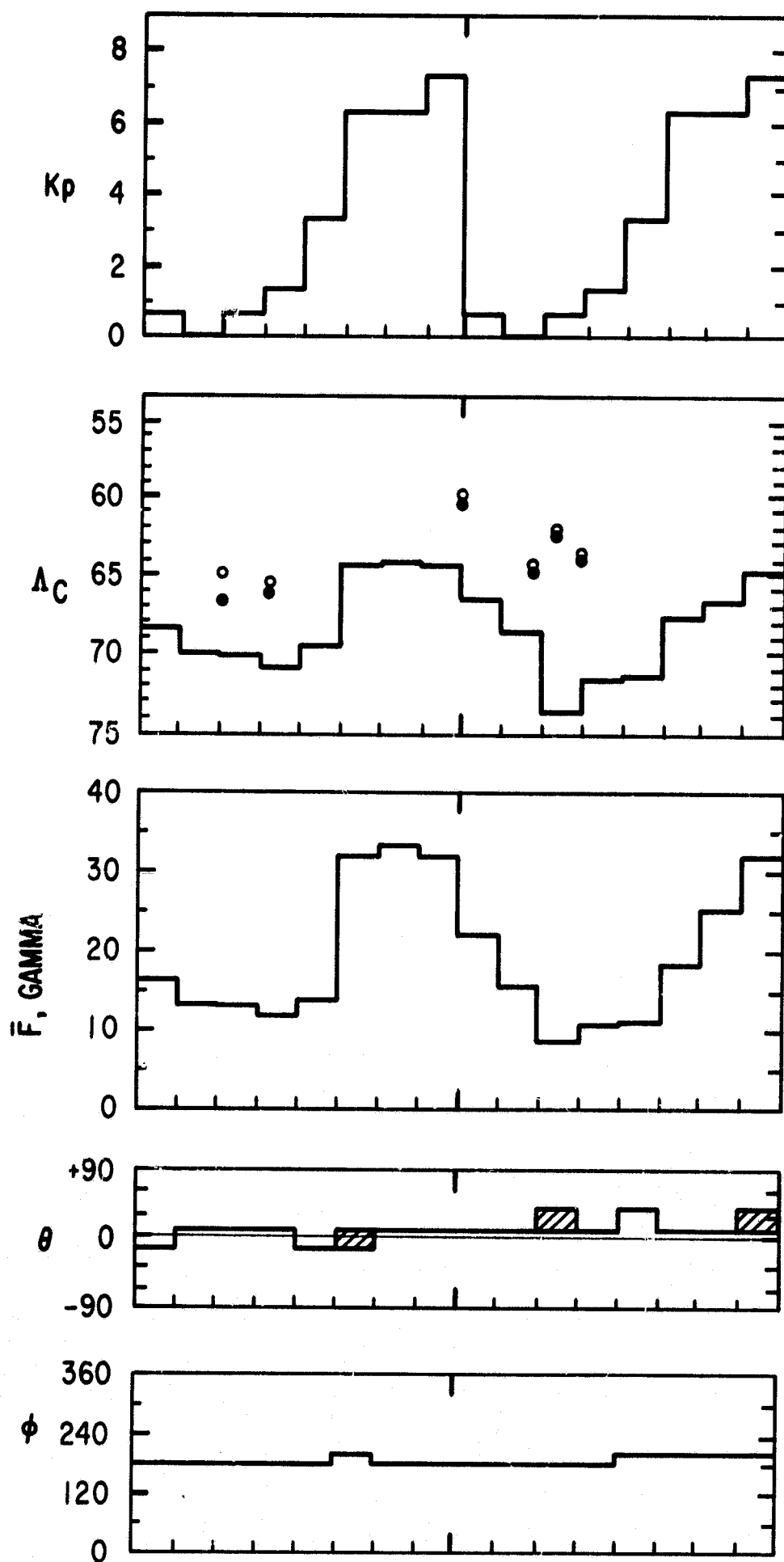


FIGURE 11





APRIL 1

APRIL 2

FIGURE 12

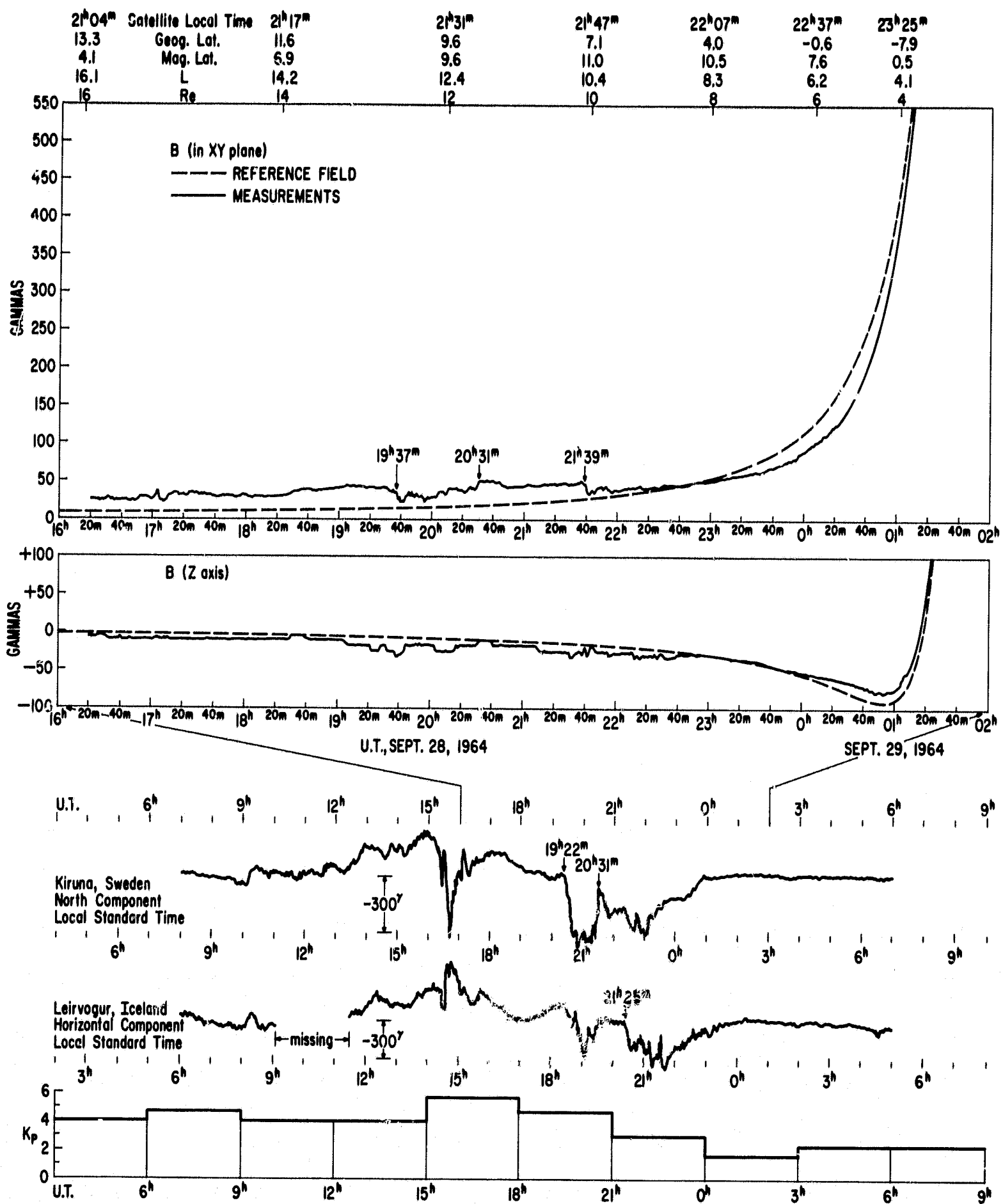


FIGURE 13

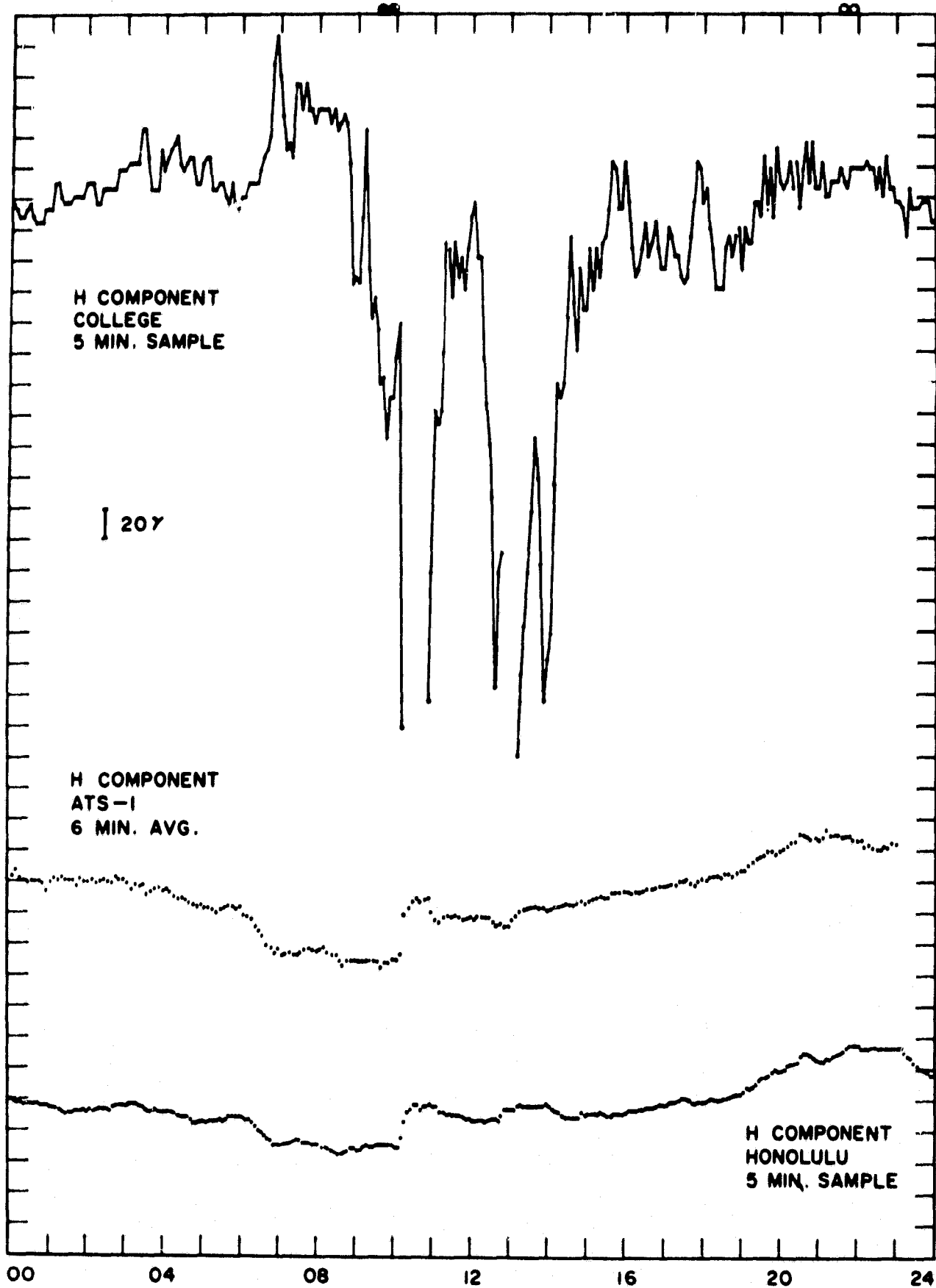


FIGURE 14